

Characteristics of dislocations at strained heteroepitaxial InGaAs/GaAs interfaces

Kevin H. Chang

Department of Materials Science and Engineering, The University of Michigan, Ann Arbor, Michigan 48109

Paliab K. Bhattacharya

Department of Electrical Engineering and Computer Science, The University of Michigan, Ann Arbor, Michigan 48109

Ronald Gibala

Department of Materials Science and Engineering, The University of Michigan, Ann Arbor, Michigan 48109

(Received 2 December 1988; accepted for publication 13 June 1989)

The formation, interaction, and propagation of misfit dislocations in molecular-beam epitaxial InGaAs/GaAs heterointerfaces have been studied by transmission electron microscopy. With the lattice mismatch less than 2%, most of the interfacial dislocations are found to be 60° mixed dislocations introduced by glide processes. Sessile edge-type dislocations can also originate from the combination of two 60° mixed dislocations. The ratio of densities of edge dislocations to 60° dislocations was increased during the later part of the elastic strain relaxation. These sessile edge dislocations may be generated in appreciable numbers through a climb process. For large lattice-mismatched systems, the majority of the misfit dislocations are pure edge dislocations and high threading dislocation density is generally found. The interfacial dislocation network is found to contain regions of dislocations with the same Burgers vector that extend over several micrometers. The results support a mechanism that involves misfit dislocation multiplication during the molecular-beam epitaxial growth process.

I. INTRODUCTION

Strained heteroepitaxial growth of semiconductors has been extensively studied in recent years.^{1,2} The accommodation of misfit strain during mismatched heterostructure epitaxy is of great importance for electronic device applications. At the same time, the generation and bowing of dislocations in thick strained layers has a critical effect on the quality of optical devices. It is generally accepted that during strained layer epitaxy the limit of coherent growth, or the pseudomorphic regime, is defined by a critical thickness. Matthews and Blakeslee³ suggested that misfit smaller than 7% can be accommodated by elastic strain until a critical thickness is reached. Above this critical thickness, it is energetically favorable for the misfit to be shared between dislocations and remnant elastic strain in the neighboring undislocated portions of the crystal. It is generally believed that when misfit dislocations are generated at a heterointerface, most, but not all, of the strain is relaxed,⁴⁻⁶ such that small residual elastic strain still exists at the misfit interface. This postulate has been confirmed by annealing experiments where it is seen that the dislocation density increases with the duration of annealing.⁷ Recently, many of the variables involved in the analysis of strain relaxation have been examined.^{8,9} The epitaxial growth temperature, dislocation line tension, lattice parameter mismatch, as well as the thickness of the overlayer, are very important factors in the generation of misfit dislocations.

Matthews proposed that substrate dislocations can act as sources of interfacial misfit dislocations through a glide process.¹⁰ The threading dislocations can bow at the hetero-

interface under the influence of misfit strain. As a result, the segments of the threading dislocation in the epilayer and the substrate will then be separated by a length of misfit dislocation within the interface to balance the stress and the dislocation line tension. It has also been suggested that dislocation multiplication processes at or near the epitaxial surface are responsible for the observed misfit dislocation substructure. For example, the formation of a dislocation half-loop near the epitaxial surface can reduce the surface steps and then grow into the misfit interface during strained epitaxial growth.¹¹⁻¹³ The surface reconstruction of semiconductors, together with the atomic growth steps, have also been considered as the possible sites for surface strain relaxation.¹⁴⁻¹⁶ In support of the former theory, a low dislocation density in the substrate (10^4 – 10^5 cm⁻²) reduces the occurrence of threading dislocations.⁷ Moreover, if threading dislocations were the only source, the strain relaxation would be limited by the dislocation glide velocity.¹⁷ In the latter theory, the rather small value of the misfit and large activation barriers oppose the nucleation of new dislocations at typical InGaAs growth temperatures ($T_g = 450$ – 550 °C) by molecular-beam epitaxy (MBE).^{4,7,17} The generation of new dislocations is impeded by the necessity to overcome the nucleation barrier. Therefore, dislocation multiplication from sources formed by the interaction of the misfit dislocations could be as important as the threading dislocations and dislocation half-loops for interfacial elastic strain relaxation.¹⁵

The aim of this paper is to study the origin of misfit dislocations during strained InGaAs layer growth on GaAs by MBE. We present results on transmission electron microscopy (TEM) investigations of misfit dislocation interac-

tion at the strained InGaAs/GaAs heteroepitaxial interface. Dislocation propagation from the heterointerface has also been studied by cross-sectional TEM. The results support a mechanism involving dislocation multiplication during MBE growth process.

II. EXPERIMENT

Molecular-beam epitaxial growth was performed in a three-chamber RIBER 2300 system. The strained InGaAs layers were grown on (001) undoped GaAs substrates. The substrates were initially solvent degreased. Mechanical damage resulting from polishing was removed by etching in a mixture of $\text{H}_2\text{SO}_4\text{:H}_2\text{O:H}_2\text{O}_2$ (5:1:1). Surface oxides on the substrates were removed by a quick etch in concentrated HCl (1:1 with water). The substrates were removed by a quick etch in concentrated HCl (1:1 with water). The substrates were then rinsed in deionized water and mounted on molybdenum sample holders with indium. Prior to growth, oxides were desorbed at 600 °C under an As_4 flux. Reflection high-energy electron diffraction (RHEED) was used to monitor desorption of the oxides. A 0.25- μm GaAs buffer layer was first grown at 600 °C, followed by 150 nm of $\text{In}_x\text{Ga}_{1-x}\text{As}$, where $x = 0.1\text{--}0.5$, grown at a rate of 1.0 $\mu\text{m/h}$ and at various substrate temperatures.

Specimens for cross-sectional TEM analysis were prepared by gluing together six $5 \times 5 \text{ mm}^2$ GaAs wafers face-to-face with epoxy, with the center two wafers containing the MBE grown structures. The wafer blocks were sliced by a diamond saw along $\langle 110 \rangle$ cleavage directions. The cross-sectional slices were ground, dimpled and then thinned to electron transparency by ion milling. Plan-view samples were dimpled from the substrate side before ion thinning. The specimens were examined in a JEOL 2000FX transmission electron microscope operating at 200 kV.

III. RESULTS AND DISCUSSION

A. Misfit dislocation networks

The general nature of the misfit dislocation network at the $\text{In}_{0.15}\text{Ga}_{0.85}\text{As/GaAs}$ interface is an asymmetrical orthogonal array as shown in Fig. 1. This asymmetry is due to the absence of inversion symmetry in the zinc-blende lattice.¹⁸ Bragg reflections responsible for the misfit dislocation image contrast are 220, 400, $2\bar{2}0$, and 040. The dislocation lines are straight because they lie at the intersection of $\{111\}$ slip planes and the (001) heterointerface and are in $[110]$ and $[1\bar{1}0]$ directions. Although pure edge dislocations with the Burgers vector lying in the heterointerface can accommodate the maximum elastic strain,³ most of the misfit dislocations are found to be mixed dislocations with Burgers vectors of $a/2\langle 110 \rangle$ type at 60° to the dislocation line. This configuration occurs because the 60° mixed dislocation can easily glide to the elastically strained interface on $\{111\}$ slip planes. The Burgers vectors of pure edge dislocations are $\pm a/2[1\bar{1}0]$ or $\pm a/2[110]$ which lie on the (001) interface, while the Burgers vector of 60° mixed dislocations are $\pm a/2[101]$, $\pm a/2[10\bar{1}]$, $\pm a/2[011]$, or $\pm a/2[0\bar{1}1]$ which are inclined from the (001) interface by 45°. Weak residual contrast of 60° mixed dislocations can be seen under

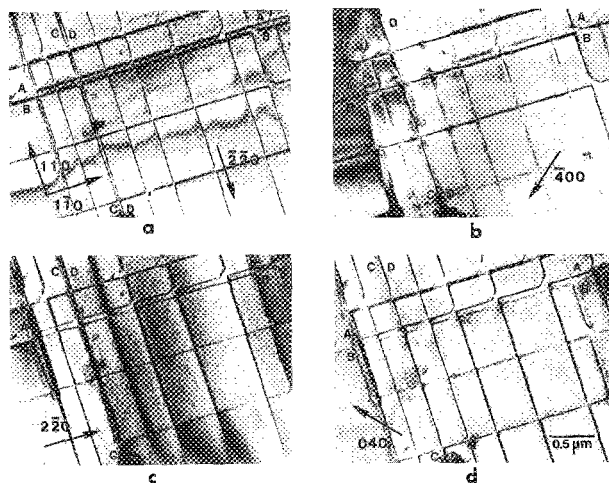


FIG. 1. Plan-view TEM micrographs of general misfit dislocations network at the InGaAs/GaAs heteroepitaxial interface formed by molecular-beam epitaxy: (a) g_{220} , (b) g_{400} , (c) $g_{2\bar{2}0}$, and (d) g_{040} .

the $(\mathbf{g}\cdot\mathbf{b}) = 0$ invisibility condition. Also, the TEM observations from a variety of sample tilts confirm that most of the misfit dislocations in the network are at the same heterointerface.

It is found that when two parallel dislocations with Burgers vectors inclined to each other by 60° are parallel as a pair, they can attract each other. Two examples of parallel dislocations, (A,B) and (C,D), are shown in Fig. 1. In Fig. 2 it is clear that some of these paired dislocations can recombine to form sessile type 90° dislocations according to the following reaction:

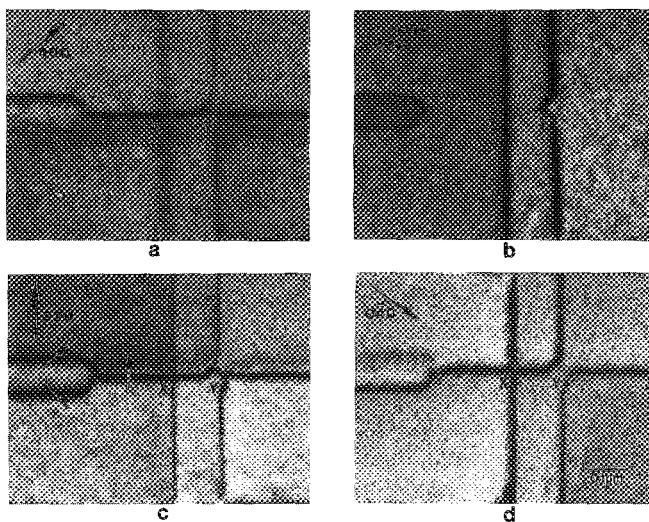
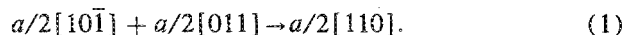


FIG. 2. Plan-view TEM micrographs of pairs of parallel mixed dislocations which recombine to form sessile edge-type dislocation. The Burgers vectors of these two mixed dislocations are inclined to each other by 60°. The micrographs also show the interaction between the pure edge dislocation and the two 60° mixed dislocation. A new 60° mixed dislocation segment, Y, is formed at the crossing point. No reaction occurs at the intersection X. The diffraction conditions are (a) g_{400} , (b) g_{220} , (c) $g_{2\bar{2}0}$, and (d) g_{040} .

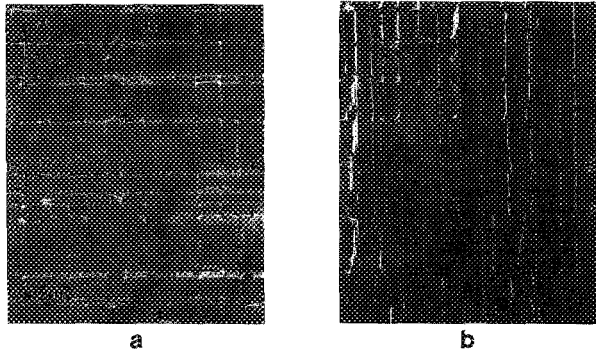
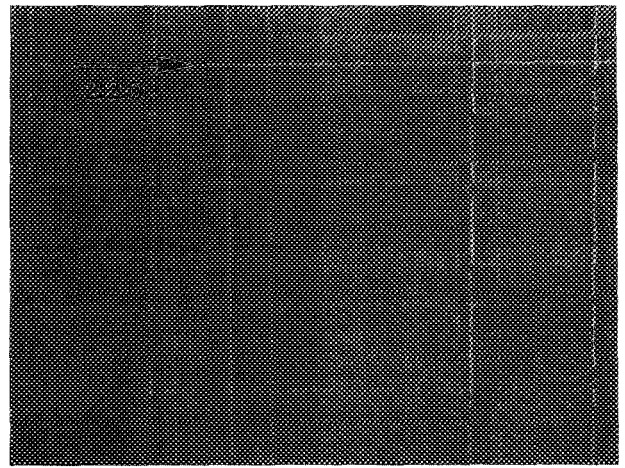


FIG. 3. Plan-view TEM micrograph of misfit dislocation network at $\text{In}_{0.2}\text{Ga}_{0.8}\text{As}/\text{GaAs}$ heteroepitaxial interface highlighting pure edge dislocations (between E and F and between H and I): (a) g_{220} and (b) g_{120} .

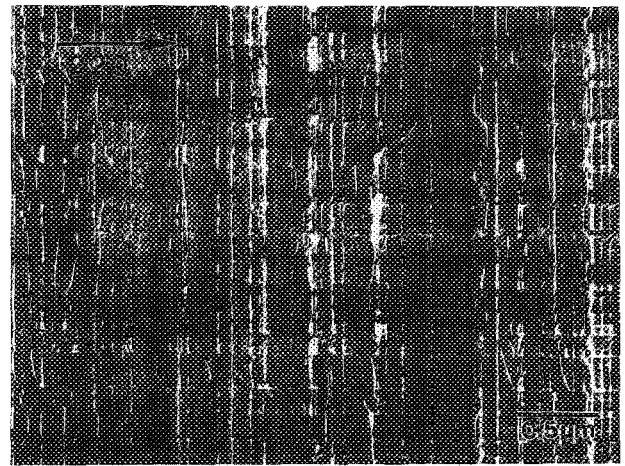
This reaction has also been observed by others using TEM and cathodoluminescence techniques.^{16,19,20} Usually these edge dislocations, generated from two mixed dislocations, were found at the early stage of strain relaxation and for relatively low mismatched systems ($< 2\%$). The details of the dislocation interactions between the pure edge and the two perpendicular mixed dislocations shown in Fig. 2 will be discussed later.

With the increase of misfit between the substrate and the epilayer, more sessile type edge dislocations are found in the interfacial dislocation network. Figure 3 shows that irregular sessile type edge dislocations are formed between two glissile 60° mixed dislocations (E,F) and (H,I) at the $\text{In}_{0.15}\text{Ga}_{0.85}\text{As}/\text{GaAs}$ interface. In order to understand the generation of these pure edge dislocations, strain relaxation in the $\text{In}_x\text{Ga}_{1-x}\text{As}$ layer of various thicknesses was studied. Figures 4(a) and 4(b) show the interfacial misfit dislocation network of $\text{In}_{0.14}\text{Ga}_{0.86}\text{As}/\text{GaAs}$ at different layer thicknesses. The pure edge misfit dislocations are found when the strained layer thickness is below 1000 \AA . As shown in Fig. 4(b) the sessile edge dislocations are generally formed in the later part of the strain relaxation process. This phenomenon has also been observed in the GaAs/Si heteroepitaxial system by Sharan *et al.*²¹ Therefore, the irregular edge dislocations shown in Fig. 3 might be generated individually after the formation of the straight 60° mixed dislocations for local strain relaxation. It is apparent that these edge dislocations are introduced by climb processes, instead of the recombination of two 60° mixed dislocations.²² Some of these edge dislocations can cross through the mixed dislocations and interact with them.

If all the elastic strain is accommodated by the misfit dislocations at the heteroepitaxial interface, the mean spacing d between the dislocations would be $\kappa b/\epsilon$,¹³ where ϵ and b are the misfit fraction and Burgers vector, respectively. The factor κ is 1 for edge dislocations, and 0.5 for 60° mixed dislocations.¹³ For complete strain relief in the $\text{In}_{0.15}\text{Ga}_{0.85}\text{As}$ layer by all 60° dislocations or all edge dislocations, the mean spacing d is approximately 200 or 400 \AA , respectively. The average dislocation spacing in Fig. 4(b) is larger than 500 \AA . This means the layer is not fully relaxed, and pure edge dislocations may be favored to accommodate the residual strain.



a



b

FIG. 4. Weak beam images show the interfacial misfit dislocation network of $\text{In}_{0.14}\text{Ga}_{0.86}\text{As}/\text{GaAs}$ heteroepitaxial interface at epilayer thicknesses of (a) 1000 \AA and (b) 2000 \AA .

In the case of $\text{In}_{0.5}\text{Ga}_{0.5}\text{As}$ on GaAs , which has about 3.5% lattice mismatch, the majority of the misfit dislocations were found to be sessile type edge dislocations. This is not only because pure edge dislocations can accommodate twice as much the elastic strain compared to 60° mixed dislocations, but also because island growth is favored during MBE of such layers.²³ For the case of island growth, pure edge dislocations are generally formed by the coalescence between two islands during the epitaxial growth.²⁴

B. Interfacial dislocation interactions

Figure 5 shows several different dislocation interactions at the $\text{InGaAs}/\text{GaAs}$ heteroepitaxial interface grown by MBE. A schematic diagram of these reactions is shown in Fig. 6. As mentioned by Abrahams *et al.*,⁶ if Burgers vectors, b_1 , combine in a way that results in an increase in elastic energy, that is

$$b_1^2 + b_2^2 < b_3^2, \quad (2)$$

no reaction will occur. At the crossing points J and K in Fig.

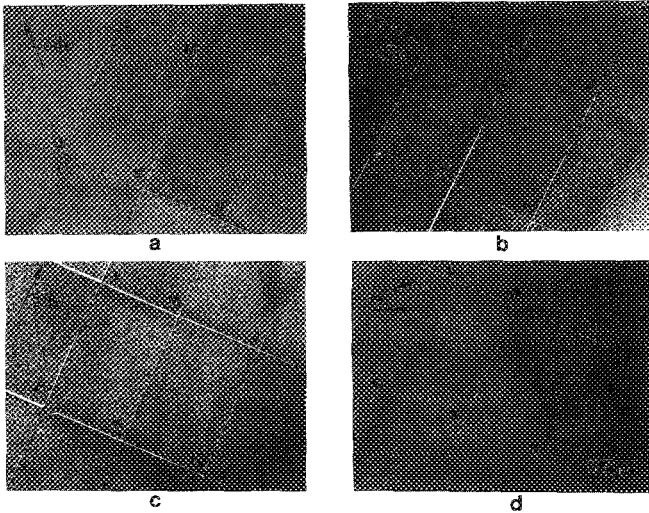


FIG. 5. Weak beam images of the dislocation interactions at the InGaAs/GaAs heteroepitaxial interface. As shown at crossing points J and K, no reaction occurs for two dislocations with perpendicular Burgers vectors. Interaction between two dislocations with 60° inclined Burgers vectors generate new screw character segments L, M, and N. The crossing point O shows two dislocations with identical Burgers vectors interacting with each other. The diffraction conditions are (a) g_{040} , (b) g_{220} , (c) $g_{2\bar{2}0}$, and (d) g_{400} .

5, no reactions are found for the two 60° mixed dislocations with perpendicular Burgers vectors. The same is also true for two orthogonal pure edge dislocations. A related configuration with an attractive dislocation junction, a triple node, can occur by the interaction of two 60° mixed dislocations with the Burgers vectors inclined to each other by 60°. Figure 5 also contains several interactions of two orthogonal 60° mixed dislocations crossing through each other. The three new dislocation segments L, M, and N generated at the intersections have screw character. Their origin is explained by Amelinckx²⁵ and Vdovin *et al.*⁷ by the reaction

$$a/2[10\bar{1}] + a/2[0\bar{1}1] \rightarrow a/2[1\bar{1}0], \quad (3)$$

$$a/2[10\bar{1}] + a/2[011] \rightarrow a/2[110], \quad (4)$$

and

$$a/2[0\bar{1}1] + a/2[\bar{1}0\bar{1}] \rightarrow a/2[\bar{1}\bar{1}0] \quad (5)$$

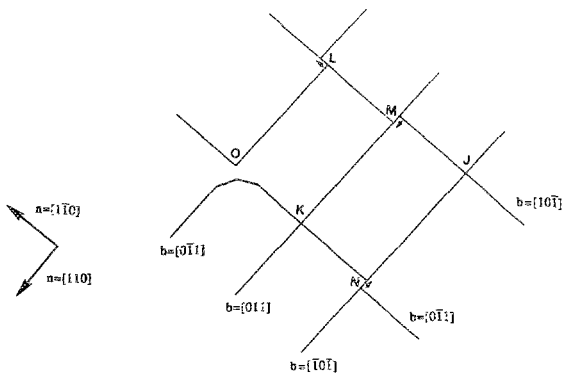


FIG. 6. Schematic illustration of the different dislocation interactions shown in Fig. 5.

for L, M, and N dislocation segments, respectively. In the case when one 60° mixed dislocation interacts with an edge dislocation, a different triple node can occur. This is seen in Fig. 2, where a new 60° mixed dislocation segment, Y, is formed by the interaction of one 60° mixed dislocation and a 90° edge dislocation by the following reaction:

$$a/2[0\bar{1}1] + a/2[110] \rightarrow a/2[101]. \quad (6)$$

In the case of the $2\bar{2}0$ reflection, the edge dislocation is practically invisible under a $(g \cdot b)_{Au} = 0$ criterion. On the other hand, no interaction occurs at intersection X. This is because the Burgers vector of the left 60° mixed dislocation has the opposite sign to the one on the right, and the reaction

$$a/2[0\bar{1}\bar{1}] + a/2[110] \rightarrow a/2[12\bar{1}], \quad (7)$$

is not favored in the zinc-blende structure.

As shown in Fig. 1 and also by other workers in different material systems,^{7,19} misfit dislocation networks exhibit a grouping behavior for dislocations with the same Burgers vector. It is most likely that the dislocations in each group, typically covering an area of at least several μm^2 , are generated from the same source. It is found that at the intersection point O in Fig. 5 two 60° mixed dislocations, each having the same Burgers vector, interact with each other to eliminate the crossing point and reduce the line energy of the dislocation.^{6,7,26} A suitable explanation of this dislocation multiplication process has been given by Hagen and Strunk.²⁷ These authors have reported that there can be a sizable repulsive interaction of two orthogonal 60° mixed dislocations with identical Burgers vectors. This repulsive reaction can lead to the formation of two angular dislocations in an asymmetric configuration. As can be seen in Fig. 7, the tip of one of the angular dislocations glides toward the film surface under the acting image force²⁷ and the dislocation line tension.⁷ After the film surface is reached, two split dislocations (P1 and Q1) with inclined screw segments at the tip are generated and can cross-slip down to the unrelaxed interfacial re-

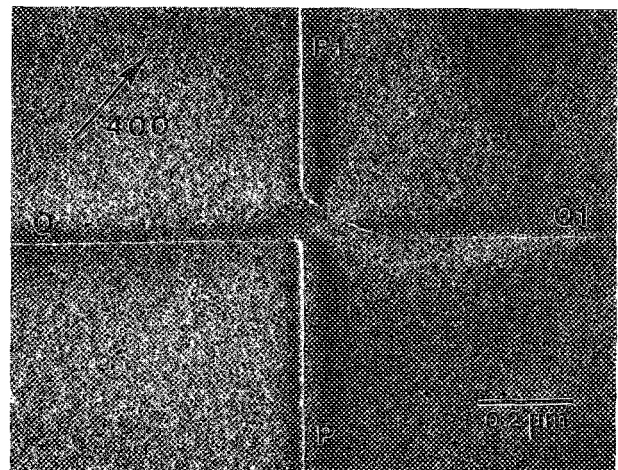


FIG. 7. TEM image of the repulsive reaction between two 60° mixed dislocations with the identical Burgers vectors. Two split dislocations with inclined screw segments are generated after the glide dislocations reach the film surface.

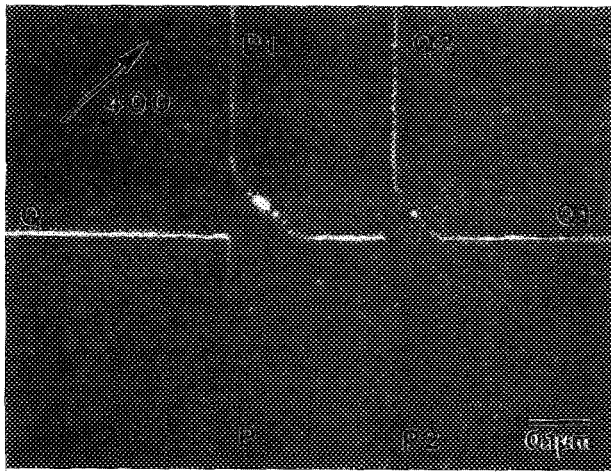


FIG. 8. Weak beam image of Hagen-Strunk-type dislocation multiplication through cross-slip processes.

gion.^{7,19} Figure 8 shows that new misfit dislocations (P2 and Q2) are then formed through a second cross-slip event. This mechanism may be repeated if the new tip of the dislocation Q1-Q2 glides to the surface.

C. Dislocation propagation from the heteroepitaxial interface

In Fig. 9(a) cross-sectional TEM micrograph reveals that few threading dislocations propagate in the $\text{In}_{0.15}\text{Ga}_{0.85}\text{As}$ epilayer region. Matthews *et al.*²⁸ suggested that the misfit strain could drive the tails of threading dislocations and dislocation half-loops to the edge of the epitaxial film to improve the layer quality. However, from the calculation of Abrahams *et al.*⁶, the linear density of misfit dislocations emerging from the edge of the heterointerface is about $2 \times 10^5 \text{ cm}^{-1}$ with $\sim 1.0\%$ misfit. If each of these misfit dislocations came from either the substrate threading dislocations or the dislocation half-loops, most of the tails of these dislocations would have to glide to the edge of the wafer without any interruption. From the dislocation interaction analysis discussed in Sec. III B, such a hypothesis seems unlikely.

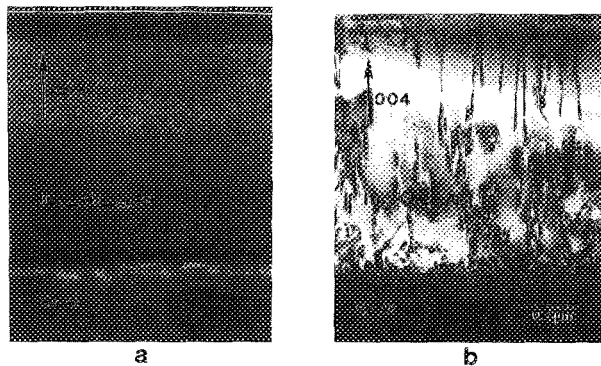


FIG. 9. Cross-sectional TEM micrograph of $\text{In}_x\text{Ga}_{1-x}\text{As}/\text{GaAs}$ heteroepitaxial structure for (a) $x = 0.15$ and (b) $x = 0.30$.

With a low dislocation density substrate and a two dimensional layer-by-layer growth mode, the multiplication by dislocations interacting with each other at the misfit interface is probably the dominant process of misfit dislocation generation. Instead of the gliding process of the dislocations from the substrate and the surface, the elastic strain relaxation could also be due to an interfacial dislocation multiplication mechanism. It was pointed out by Frank²⁹ many years ago that dislocations may be formed by dynamic multiplication processes. Classical Frank-Read sources either at the growth surface or at the heteroepitaxial interface were proposed as the mechanisms responsible for the dislocation multiplication.^{16,18,30,31} No evidence of this mechanism has been found in the $\text{InGaAs}/\text{GaAs}$ single heterostructure or $\text{InGaAs}/\text{GaAs}$ strained multi-quantum wells³² grown by MBE in our laboratory. The current results suggest that the multiplication model proposed by Hagen and Strunk is the most probable mechanism for the formation of the $\text{InGaAs}/\text{GaAs}$ interfacial misfit dislocation network.

The split of the L-shape mixed dislocation by gliding, as shown in Fig. 7, has rarely been seen for $\text{In}_{0.15}\text{Ga}_{0.85}\text{As}$ layer thickness above 1500 \AA . Therefore, as the $\text{In}_{0.15}\text{Ga}_{0.85}\text{As}$ layer thickness increases, the Hagen-Strunk dislocation multiplication mechanism may become inoperative. The sessile-type dislocations are then favored because they are more efficient in the accommodation of misfit strain. It may be suggested that the process of forming these sessile edge dislocations is probably controlled by the gliding velocity of the 60° mixed dislocations.

Figure 9(b) shows that numerous grown-in threading dislocations are in the $\text{In}_{0.3}\text{Ga}_{0.7}\text{As}$ epilayer. Most of these threading dislocations are screw type or 60° dislocations and the propagating directions are found to be close to the normal to the favored over layer-by-layer growth for large lattice mismatched systems. In addition to the gliding process of mixed dislocation and operation of the Hagen-Strunk dislocation multiplication mechanism, pure edge dislocation generation through the merging of islands become important during MBE growth. The interfacial strained relaxation process becomes much more complicated and the relaxation rate increases significantly. The completion of a dislocation gliding process at the interface and a Hagen-Strunk multiplication mechanism become very difficult. The tails of the dislocation half-loop and the transition dislocation segments of the multiplication process then thread up along the growth front.²¹ Sessile-type edge dislocations can also thread up through the climb process. Therefore, as the mismatch percentage increases, more and more threading dislocations are found in the strained epitaxial layers.

IV. SUMMARY AND CONCLUSIONS

We have shown by detailed TEM analysis the formation, interaction and propagation of misfit dislocations at an MBE-grown $\text{InGaAs}/\text{GaAs}$ heteroepitaxial interface. With the strain systems less than 2% lattice mismatch, the majority of the misfit dislocations are confined at the same heterointerface after the elastic strain relaxation. Most of the misfit dislocations are found to be mixed dislocations with Burgers vector of $a/2\langle 110 \rangle$ type at 60° to the dislocation

line. Sessile type edge dislocations can also originate from the combination of two 60° mixed dislocations. Numerous sessile edge dislocations were generated during the later part of the elastic strain relaxation through climb or interaction processes. The interfacial dislocation network is found to contain regions of dislocation with the same Burgers vector that extend over several micrometers. The interfacial dislocation multiplication process proposed by Hagen and Strunk is the most probable mechanism for this grouping character of the misfit dislocations.

For large lattice-mismatched systems ($\epsilon \gg 2\%$), the majority of the misfit dislocations are pure edge dislocations. This process occurs because island growth is favored over two-dimensional layer-by-layer growth, and the edge dislocations are often formed by island coalescence at the initial epitaxial growth. A high threading dislocation density in the InGaAs layer is generally found in the large mismatched systems. We believe this may be due to the threading of the tails of the dislocation half loop and the transition dislocation segments of a Hagen-Strunk multiplication process. In conclusion, it is apparent that very low threading dislocation density In_xGa_{1-x}As films with $x < 0.2$ can be grown on GaAs by MBE when the dislocation multiplication mechanism operates. From the understanding of the interfacial dislocation multiplication process, new growth parameters can be developed, which will be useful for realizing heterostructure devices with large mismatch.

ACKNOWLEDGMENTS

The authors gratefully acknowledge the discussions with Professors D. Srolovitz, D. C. Van Aken, and Dr. J. F. Mansfield. The work is being supported by the Department of Energy under Grant No. DE-FG02-86ER45250.

- ¹G. C. Osburn, *J. Vac. Sci. Technol. B* **1**, 379 (1983).
²P. L. Gourley and R. M. Biefeld, *J. Vac. Sci. Technol. B* **1**, 383 (1983).
³J. W. Matthews and A. E. Blakeslee, *J. Cryst. Growth* **27**, 118 (1974).
⁴J. H. van der Merwe, *J. Appl. Phys.* **34**, 117 (1963); **34**, 123 (1963).

- ⁵W. A. Jesser and D. Kuhlmann-Wilsdorf, *Phys. Status Solidi* **19**, 95 (1967).
⁶M. S. Abrahams, L. R. Weisberg, C. J. Buicchi, and J. Blanc, *J. Mater. Sci.* **4**, 223 (1969).
⁷V. I. Vdovin, L. A. Matveeva, G. N. Semenova, M. Ya. Skorohod, Yu. A. Tkhorik, and L. S. Khazan, *Phys. Status Solidi A* **92**, 379 (1985).
⁸J. Y. Tsao, B. W. Dodson, S. T. Picraux, and D. M. Cornelison, *Phys. Rev. Lett.* **59**, 2455 (1987).
⁹R. Huil, J. C. Bean, D. J. Werder, and R. E. Leibenguth, *Appl. Phys. Lett.* **52**, 1605 (1988).
¹⁰J. W. Matthews, *Philos. Mag.* **13**, 1207 (1966).
¹¹J. W. Matthews, S. Mader, and T. B. Light, *J. Appl. Phys.* **41**, 3800 (1970).
¹²J. W. Matthews, *J. Vac. Sci. Technol.* **12**, 126 (1975).
¹³G. R. Booker, J. M. Titchmarsh, J. Fletcher, D. B. Darby, M. Hockly, and M. Al-Jassim, *J. Cryst. Growth* **45**, 407 (1978).
¹⁴D. L. Rode, *Phys. Status Solidi A* **32**, 425 (1975).
¹⁵J. S. Ahearn, C. Laird, and C. A. B. Ball, *Thin Solid Films* **42**, 117 (1977).
¹⁶J. S. Ahearn and C. Laird, *J. Mater. Sci.* **12**, 699 (1977).
¹⁷B. W. Dodson, *Appl. Phys. Lett.* **53**, 394 (1988).
¹⁸M. S. Abrahams, J. Blanc, and C. J. Buicchi, *Appl. Phys. Lett.* **21**, 185 (1972).
¹⁹H. Strunk, W. Hagen, and E. Bauser, *Appl. Phys.* **18**, 67 (1979).
²⁰E. A. Fitzgerald, D. G. Ast, Y. Ashizawa, S. Akbar, and L. F. Eastman, *J. Appl. Phys.* **64**, 2473 (1988).
²¹S. Sharan, J. Narayan, and K. Jagannadham, *Abstracts of the Materials Research Society Winter Meeting*, p. 80 (1988).
²²Y. Fukuda, Y. Kohama, M. Seki, and Y. Ohmachi, *Jpn. J. Appl. Phys.* **27**, 1593 (1988).
²³P. R. Berger, K. Chang, P. Bhattacharya, J. Singh, and K. K. Bajaj, *Appl. Phys. Lett.* **53**, 684 (1988).
²⁴C. J. Kiely, J.-I. Chyi, A. Rockett and H. Morkoc, *Abst. Mat. Res. Soc. Winter Meeting*, p. 470 (1988).
²⁵S. Amelinckx, *Dislocations in Solids*, edited by F. R. N. Nabarro (North-Holland, New York, 1979), Vol. 2, p. 435.
²⁶K. Rajan and M. Denhoff, *J. Appl. Phys.* **62**, 1710 (1987).
²⁷W. Hagen and H. Strunk, *Appl. Phys.* **17**, 85 (1978).
²⁸J. W. Matthews, A. E. Blakeslee, and S. Mader, *Thin Solid Films* **33**, 253 (1976).
²⁹F. C. Frank, *Symp. on Plastic Deformation of Crystalline Solids* (Carnegie Institute of Tech. Pittsburgh, 1950), p. 89.
³⁰M. S. Abrahams, C. J. Buicchi, and G. H. Olsen, *J. Appl. Phys.* **46**, 4259 (1975).
³¹C. Herbeaux, J. Di Persio, and A. Lefebvre, *Appl. Phys. Lett.* **54**, 1004 (1989).
³²K. H. Chang, P. K. Bhattacharya, and R. Gibala, *J. Appl. Phys.* **65**, 3391 (1989).